JOURNAL OF SPACECRAFT AND ROCKETS
Vol. 56, No. 1, January–February 2019

Fengyun-4 Attitude Control System Design and Its In-Flight Performance

Liang Tang,* Shoulei Chen,† Kai Wang,‡ and Yiwu Liu§
Beijing Institute of Control Engineering, 100094 Beijing, People's Republic of China

DOI: 10.2514/1.A34226

Fengyun-4, launched on 11 December 2016, is a second-generation geostationary meteorological satellite that employs a three-axis-stabilized attitude control strategy with a zero-momentum state. This Paper introduces the attitude control system of the spacecraft platform and its in-flight performance. The development status of current meteorological satellites in the same generation are reviewed. The Fengyun-4 attitude control system and technical details are presented, including highly accurate attitude determination, attitude-pointing control with high accuracy and stability requirements under the disturbance of rapid steering payloads, momentum management and adjustment, and accommodation to operate after turning 180 deg about the yaw axis, as well as fault diagnosis, isolation, and recovery. In-flight results are presented to demonstrate that the attitude control system of the spacecraft platform could fulfill the Fengyun-4 mission requirements.

I. Introduction

FENGYUN-4 is a second-generation Chinese geostationary quantitative remote sensing meteorological satellite that employs a zero-momentum three-axis-stabilized attitude control strategy using momentum wheels. It was launched to replace the first-generation satellites, which use a spin-stabilized attitude control system. The main payloads of Fengyun-4 include the multichannel scanning radiometer, the atmospheric sounding interferometer, the lightning mapping imager, and the space environment monitoring instrument package. These instruments impose demanding requirements on the attitude control system of the spacecraft platform.

Fengyun-4 was 5400 kg in weight during prelaunch time, is capable of 3200 W of power generation at the end of its lifetime, and has a seven-year design service life. This spacecraft was delivered to a geostationary transfer orbit on 11 December 2016 and then located at 99.5°E for normal operation after five orbit maneuvers at the apsis and two phase capture maneuvers in the quasi-geosynchronous orbit.

Many challenges are encountered during the development of an attitude control system of the spacecraft platform for geostationary quantitative remote sensing. First, the high accuracy requirement on attitude determination (3 arc seconds, 3σ, per axis, random noise, relative to the inertial frame), attitude-pointing accuracy (0.01 deg, 3σ, per axis, relative to the orbital frame), and attitude-pointing stability (5×10^{-4} deg, the maximum change in angle during any given 1 s interval, per axis, relative to the orbital frame) are imposed for acquiring high-quality meteorological data. Second, Fengyun-4 has a single solar array with an area of 17 m^2, a 6 m magnetometer mechanism, and four liquid fuel tanks installed in parallel, leading to complex attitude dynamics with various types of disturbances closely interacting. Third, because the main payloads, including the multichannel scanning radiometer and the atmospheric sounding interferometer, use double-scanning mirrors to acquire meteorological data, the rapid steering motions of the scanning mechanisms disturb the spacecraft attitude in both the roll and yaw axes and have a considerable impact on the performance of the spacecraft attitude-pointing accuracy and stability in regular remote sensing operations. Fourth, the spacecraft is required to autonomously manage the momentum of each wheel and daily adjust them in a predetermined time; autonomously diagnose and dispose fault in various types of attitude sensors and actuators; and be adapted to the operation after turning around 180 deg on the yaw axis by modifying the strategy of attitude determination, station keeping, and momentum management and adjustment, to ensure that the meteorological operations can continuously and steadily run during a long period of time. The requirements of the Fengyun-4 spacecraft attitude control system are introduced in [1]. The in-flight configuration of the Fengyun-4 spacecraft and its body-fixed frame are shown in Fig. 1.

The organization of this Paper is as follows. First, the spacecraft attitude control systems of the geostationary meteorological spacecraft belonging to the same generation as that of Fengyun-4 are introduced. Second, the system architecture and critical techniques of the Fengyun-4 spacecraft attitude control system are presented in detail. Third, the telemetry results are provided to evaluate the in-flight performance of its platform attitude control system.

II. Current Status of Geostationary Meteorological Spacecraft Attitude Control System

Geostationary Operational Environmental Satellite-R series (GOES-R), Himawari 8/9, and Meteosat Third Generation (MTG) are usually classified as the new generation of geostationary meteorological spacecraft. The requirements and architecture of their spacecraft attitude control system are nearly the same as the Fengyun-4 spacecraft. The technical statuses of the three geostationary meteorological spacecraft are briefly introduced as follows.

The GOES-R spacecraft is the first of the next-generation United States meteorological spacecraft and was launched on 19 November 2016. This spacecraft has significant improvements in the resolution, observation rate, and spectral bands for Earth observations in comparison with its old system. With a single solar array on its south panel, this spacecraft adopts a three-axis-stabilized attitude control strategy by using six reaction wheels and was designed for a 15 year mission duration. A three-head star tracker and two inertial reference units with four hemispherical resonator gyros each are used for high-accuracy attitude determination. An onboard global positioning

Received 21 February 2018; revision received 6 June 2018; accepted for publication 10 June 2018; published online 24 September 2018.

*Researcher; currently Key Laboratory of Space Intelligent Control Technology, 100094 Beijing, People's Republic of China; tl614@sina.com.

†Senior Engineer; currently Key Laboratory of Space Intelligent Control Technology, 100094 Beijing, People's Republic of China; chenshi8848@sina.com.

‡Engineer; currently Key Laboratory of Space Intelligent Control Technology, 100094 Beijing, People's Republic of China; wkwk20047@163.com (Corresponding Author).

§Researcher; currently Key Laboratory of Space Intelligent Control Technology, 100094 Beijing, People's Republic of China; liuyiwu_615@sohu.com.

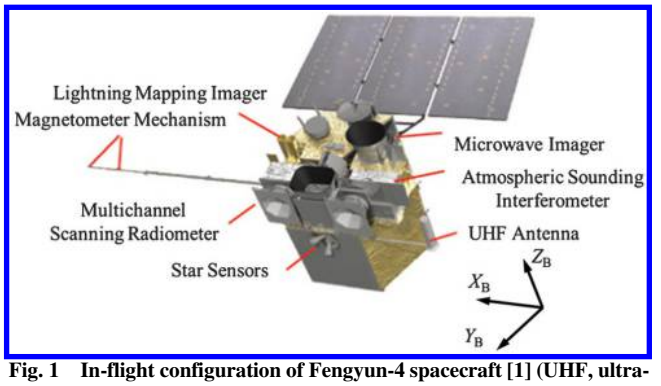

Fig. 1 In-flight configuration of Fengyun-4 spacecraft [1] (UHF, ultra-high frequency).

system receiver is selected to replace the traditional ground upload method and could provide highly accurate orbital positions and velocities. Active vibration damping and passive isolation techniques are employed to mitigate various types of disturbance sources and satisfy the attitude-pointing stability requirements, 0.09 N low-thrust thrusters are used for momentum adjustment and east–west station keeping, and 0.2 N arcjet thrusters are used for north–south station keeping. Six reaction wheels are used for high-accuracy attitude-pointing control and can feed forward the thruster torques during daily momentum adjustment events and frequent station-keeping maneuvers as well as the disturbance torques induced by the rapid motion of the scanning mirrors. The lost observation time caused by exceeding the attitude-pointing and stability requirements is less than 120 min per year. Its specific techniques and the in-flight performance of its attitude control system are presented by Chapel et al. in [2,3].

Himawari 8 and 9 spacecraft are the third-generation geostationary meteorological spacecraft of Japan and were launched on 7 October 2014 and 2 November 2016, respectively. These two spacecraft provide meteorological observation service for the East Asia and Western Pacific areas. The spacecraft have a single solar array and choose a three-axis-stabilized attitude control strategy with bias momentum provided by four momentum wheels. The spacecraft have a lifespan of 15 years and can be operated for meteorological service for 8 years. The Himawari 8 and 9 spacecraft are equipped with various types of attitude sensors. Coarse sun sensors are used for establishing the initial attitude state and pointing the solar array toward the sun during the safety mode. Two star trackers in cooperation with inertial reference units are used for high-accuracy attitude determination, and angular rate sensors are employed for measuring the high-frequency vibration. Its primary science instrument Advanced Himawari Imager is similar to that used in the GOES-R spacecraft [4]. Its mission overview and the system architecture can be found in [5,6].

MTG spacecraft are the third-generation geostationary meteorological satellites in Europe and are composed of six spacecraft. Four spacecraft are used for imaging observation, and the other two are used for sounding applications. Those spacecraft use a three-axis-stabilized attitude control strategy and have a lifespan of 8.5 years. Double solar arrays are adopted to reduce the angular momentum accumulation generated by solar pressure. The spacecraft can turn around 180 deg on the yaw axis to avoid the $-Y$ panel exposure to the sun. High-precision gyroscopes and a multihead star tracker are used in the MTG satellites to achieve the high-accuracy attitude determination requirement. Five reaction wheels are employed to achieve the high-accuracy attitude-pointing requirement and compensate the attitude disturbance generated by the steering motion of the payloads. The mission overview and the system architecture can be found in [7,8].

III. System Architecture and Specific Techniques of Fengyun-4 Spacecraft Attitude Control System

This Paper focuses exclusively on the Fengyun-4 attitude control system of the spacecraft platform. Additional information about its image navigation and registration system as well as its vibration isolation system can be founded in [9,10]. The requirements on the Fengyun-4 attitude control system are present in Table 1. The architecture of the Fengyun-4 attitude control system is shown in Table 2. To meet the requirements mentioned previously, some specific techniques in the control system are presented as follows.

A. High-Accuracy Attitude Determination

Three high-accuracy star trackers are used to measure the attitude of the body-fixed frame relative to the inertial frame. The star sensors are installed centrally on the $+Y$ panel. The misalignment of the star sensors caused by thermal distortion are considerably mitigated via highly efficient thermal control and maintaining a 0 or 180 deg attitude along the yaw axis to avoid solar radiation. The absolute and relative installation errors of the star trackers are compensated in the control system to improve the accuracy of the attitude determination. The inertial attitude of the spacecraft and the drifts of the gyroscopes are estimated based on a constant gain Kalman filter [11]. The measurement information includes the inertial information provided by the star trackers and the angular velocities obtained from high-accuracy gyroscopes. The relative attitude angles between any two star trackers are calculated based on their inertial outputs or their installation matrix in the body-fixed frame. The control system compares those two pieces of information to ensure that the attitude determination filter can use the validated outputs of the star trackers and has a steady-going state. A backup algorithm for attitude determination is proposed in case those gyroscopes are disabled. Attitude dynamics and torques generated by the thrusters, momentum wheels, solar radiation, and motion of the payloads are calculated in that algorithm. Together with the attitude dynamics model of the spacecraft and the outputs of the star trackers, the inertial attitude and the angular velocity of the spacecraft are estimated by a constant gain Kalman filter. The algorithm has a tolerable performance on the attitude determination accuracy. The performance of those two algorithms can be evaluated by the numerical simulations with a high-fidelity model. The attitude determination errors are present in Figs. 2 and 3. Statistical results suggest that the attitude determination errors based on the star trackers and gyroscopes reach 1.5×10^{-4} deg (1.62 arc seconds, 3σ), while the errors based on the star trackers and attitude dynamics reach 2.9×10^{-4} deg (3.13 arc seconds, 3σ).

The constant gain Kalman filters output the attitude quaternion $\boldsymbol{q}_{\mathrm{BI}}$ and the angular velocity $\boldsymbol{\omega}_{\mathrm{BI}}$ of the spacecraft body-fixed frame relative to the inertial frame. Then, together with the orbital

Table 1 Requirement on the Fengyun-4 attitude control system

Requirement	Value	Error Source
Attitude determination accuracy (3σ, per axis, relative to the inertial frame)	0.0056 deg	Absolute installation error; Residual error of low frequency misalignment; Random noise;
Attitude-pointing accuracy (3σ, per axis, relative to the orbital frame)	0.01 deg	Attitude determination accuracy; Orbit determination error; Time error; Attitude control error;
Attitude-pointing stability (the maximum change in angle during any given 1 s interval, per axis, relative to the orbital frame)	5×10^{-4} deg	
Convergence time of the daily momentum adjustment	<15 min	
Yaw flip maneuvers (accommodation to the inverse attitude)	Twice per year	

Table 2 Architecture of the Fengyun-4 attitude control system

Components	Device
Attitude control computer	Control computer (2 computers with 1 cold spare); Fault-tolerant circuit (monitoring the working state of the control computer and realizing the fault-tolerant control logic of the control computer); Emergency circuit (making the spacecraft point to the sun while the control computer cannot operate normally)
Sensors	9 gyroscopes; 4 digital sun sensors; 2 infrared Earth sensors; 3 star sensors
Actuators	6 momentum wheels (50 N · m · s); 1 solar array drive assembly; 18 thrusters (10 N); 1 apogee engine (490 N)

determination information, the attitude information of the spacecraft body-fixed frame relative to the orbital frame can be calculated as

$$\begin{aligned} \boldsymbol{q}_{\mathrm{BO}} &= \boldsymbol{q}_{\mathrm{OI}}^{-1} \otimes \boldsymbol{q}_{\mathrm{BI}} \\ \boldsymbol{\omega}_{\mathrm{BO}} &= \boldsymbol{\omega}_{\mathrm{BI}} - \boldsymbol{C}_{\mathrm{BO}}(\boldsymbol{q}_{\mathrm{BO}})\boldsymbol{\omega}_{\mathrm{OI}} \end{aligned} \tag{1}$$

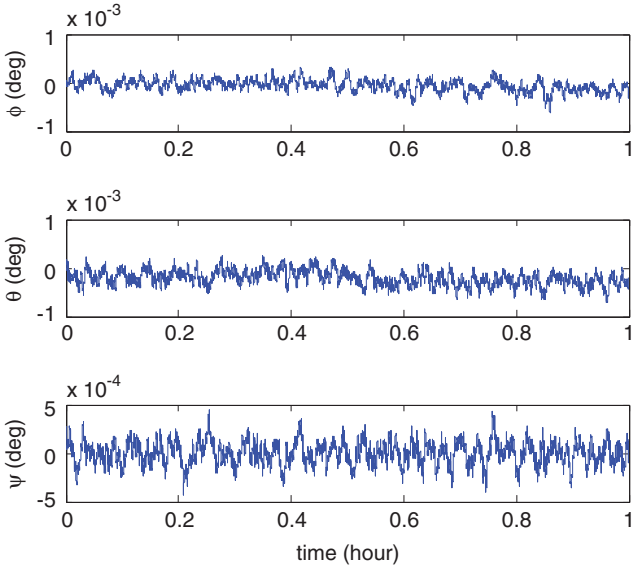

Fig. 2 Attitude determination errors based on star trackers and gyroscopes.

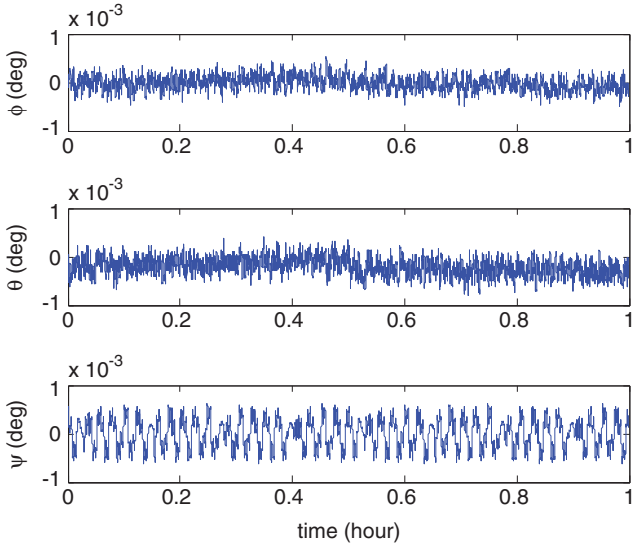

Fig. 3 Attitude determination errors based on star trackers and attitude dynamics.

where $\boldsymbol{q}_{\mathrm{BO}}$ and $\boldsymbol{\omega}_{\mathrm{BO}}$ are the attitude quaternion and the angular velocity of the spacecraft body-fixed frame relative to the orbital frame; $\boldsymbol{q}_{\mathrm{OI}}$ and $\boldsymbol{\omega}_{\mathrm{OI}}$ are the attitude quaternion and the angular velocity of the orbital frame relative to the inertial frame; $\boldsymbol{C}_{\mathrm{BO}}$ is the attitude transition matrix from the orbital frame to the spacecraft body-fixed frame; and $\boldsymbol{q}_{\mathrm{OI}}$, $\boldsymbol{\omega}_{\mathrm{OI}}$, and $\boldsymbol{C}_{\mathrm{BO}}$ can be calculated by the orbital determination information.

There exist low-frequency changes between the measurement frame of the star trackers and that of the payloads because of the influence of the thermal distortion. To solve that problem, Fengyun-4 uses a least-square method to estimate the low-frequency misalignment based on the geometric relationship between the spacecraft and the landmark on Earth [12]. The measurement information contains the orientation of the landmark observed by the payloads as well as the orbit and attitude information of the spacecraft. The misalignment angle in each axis is divided into two parts: the constant component and the periodic component. The estimated coefficients and the periods are uploaded to the control system to compensate the misalignment errors in real time.

The least-square equation mentioned previously has the form

$$\begin{bmatrix} \boldsymbol{\theta}_x \\ \boldsymbol{\theta}_y \\ \boldsymbol{\theta}_z \end{bmatrix}_{21\times 1} = (\boldsymbol{\Phi}^T\boldsymbol{\Phi})^{-1}\boldsymbol{\Phi}^T \begin{bmatrix} \boldsymbol{r}_{M1} - \hat{\boldsymbol{r}}_{B1} \\ \boldsymbol{r}_{M2} - \hat{\boldsymbol{r}}_{B2} \\ \vdots \\ \boldsymbol{r}_{Mn} - \hat{\boldsymbol{r}}_{Bn} \end{bmatrix}_{3n\times 1} \tag{2}$$

where $\boldsymbol{r}_{Bi}$ $(i = 1, 2, \ldots, n)$ are the unit vectors from the spacecraft to the landmark, which is observed by the Earth observation payload and described in its measurement frame; $\hat{\boldsymbol{r}}_{Bi}$ $(i = 1, 2, \ldots, n)$ are the unit vectors from the spacecraft to the landmark described by the body frame, which is calculated based on the relative position vectors from the spacecraft to the landmark in the inertial frame as well as the inertial attitude obtained by the star trackers.

The estimated coefficients of the misalignment between the spacecraft body frame and the payload measurement frame are denoted by $\boldsymbol{\theta}_x, \boldsymbol{\theta}_y, \boldsymbol{\theta}_z$ and, which consists of the constant coefficient c_{i0} $(i = x, y, z)$ and the periodic coefficients $\alpha_{i1}, \beta_{i1}, \alpha_{i2}, \beta_{i2}, \alpha_{i3}$, and β_{i3} $(i = x, y, z)$ related to one to approximately three times orbital period, respectively.

Φ is the state transition matrix and has the form

$$\begin{aligned} \boldsymbol{\Phi} &= \begin{bmatrix} 2\hat{\boldsymbol{r}}_{B1}^{\times}\boldsymbol{\varphi}_1 \\ 2\hat{\boldsymbol{r}}_{B2}^{\times}\boldsymbol{\varphi}_2 \\ \vdots \\ 2\hat{\boldsymbol{r}}_{Bn}^{\times}\boldsymbol{\varphi}_n \end{bmatrix}_{3n\times 21} \\ \boldsymbol{\varphi}_k &= \begin{bmatrix} 1 & \cos(2\pi t/T_{\mathrm{orb}}) & \sin(2\pi t/T_{\mathrm{orb}}) & \cos(4\pi t/T_{\mathrm{orb}}) \\ & \sin(4\pi t/T_{\mathrm{orb}}) & \cos(6\pi t/T_{\mathrm{orb}}) & \sin(6\pi t/T_{\mathrm{orb}}) \end{bmatrix} \end{aligned} \tag{3}$$

where T_{orb} is the orbital period.

Additionally, a similar estimation method is adopted to estimate the low-frequency changes based on the orientations of the stars in the Earth disk background observed by the payload. The Fengyun-4 high-accuracy attitude determination method is illustrated in Fig. 4.

B. Attitude-Pointing Control with High Accuracy and Stability

Based upon the high-accuracy attitude determination approach mentioned previously, Fengyun-4 employs momentum wheels to maintain a three-axis-stabilized attitude and feed forward the disturbance torques to fulfill the requirement in attitude-pointing accuracy and stability of the spacecraft platform. The two main payloads, namely, the multichannel scanning radiometer and the atmospheric sounding interferometer, adopt double-scanning mirrors to accomplish east–west and north–south scanning motion and have multiple functional modes, such as scanning, pointing, and calibration. The momenta of inertia of the moving mechanism in those two main payloads are 0.06 (east–west mirrors) and 0.2 kg · m^2

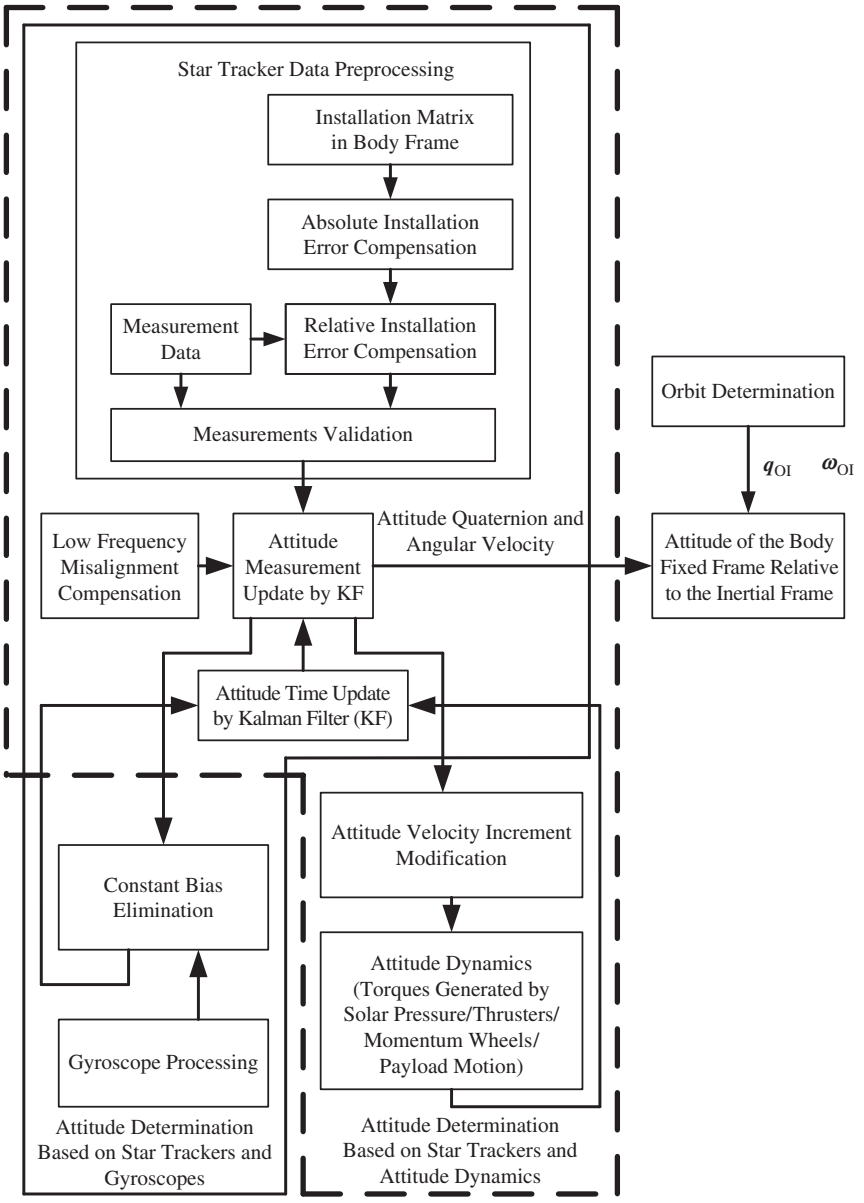

Fig. 4 High-accuracy attitude determination approach (KF, Kalman filter).

(north–south mirrors). Prelaunch analysis and simulations suggest that the attitude-pointing stability of the spacecraft becomes worse when the mechanisms have a large angular movement in the fast pointing functional mode. In particular, the motion of the north–south scanning mirror could result in the attitude-pointing stability around the *X* axis of the body-fixed frame exceeding the mission requirement. (In that case, the maximum disturbance torque is 0.1097 N · m, and the maximum disturbance angular momentum is 0.0349 N · m · s) For that reason, the Fengyun-4 spacecraft uses a feedforward control strategy implemented by momentum wheels to autonomously compensate the angular momentum changes that arise from the double-scanning mirrors making accelerated and decelerated motions. Its performance is evaluated by numerical simulations, and the results can be found in Figs. 5–9. As shown in Figs. 5 and 6, the east–west scanning mirror in the multichannel scanning radiometer has a periodic motion, and the scanning mirrors in the atmospheric sounding interferometer begin to make fast pointing motions at 100 s. Figure 7 presents the feedforward torques generated by momentum wheels to compensate those periodic and fast pointing motions. The feedforward torque along the *X* axis is mainly used to compensate the fast pointing motion of the north–south scanning mirror in the atmospheric sounding interferometer. The feedforward torque along the *Z* axis is mainly used to compensate the periodic motion of the east–west scanning mirror in the multichannel scanning radiometer. Figures 8 and 9 suggest that a fast pointing motion results in significant attitude errors and attitude rate errors. However, the attitude-pointing accuracy and the attitude-pointing stability of the spacecraft platform fulfill the mission requirements.

As shown in Fig. 10, payload motion commands are continuously uploaded from ground stations to the data management computer in the spacecraft and then are distributed to the attitude control system and the payloads before being conducted. After receiving those payload motion commands, the attitude control system recognizes the functional mode of the payloads and computes the compensation parameters for the feedforward control. Once the payload begins to operate in that functional mode, the attitude control system calculates the angular motion states of the scanning mirrors and then determines the feedforward torques in real time to compensate the disturbance angular momentum generated by the payloads. In combination with the feedback torques, the feedforward torques are allocated to each momentum wheel and then the spacecraft can maintain its attitude pointing to Earth. The payloads obey the motion commands and precisely drive the scanning mirrors according to the desired angles. The payloads generate the synchronization signals when the mirrors reaching some certain angles. Then the data management computer sent those signals to the attitude control system. Those signals are used to coordinate the payload motion, the imaging compensation in

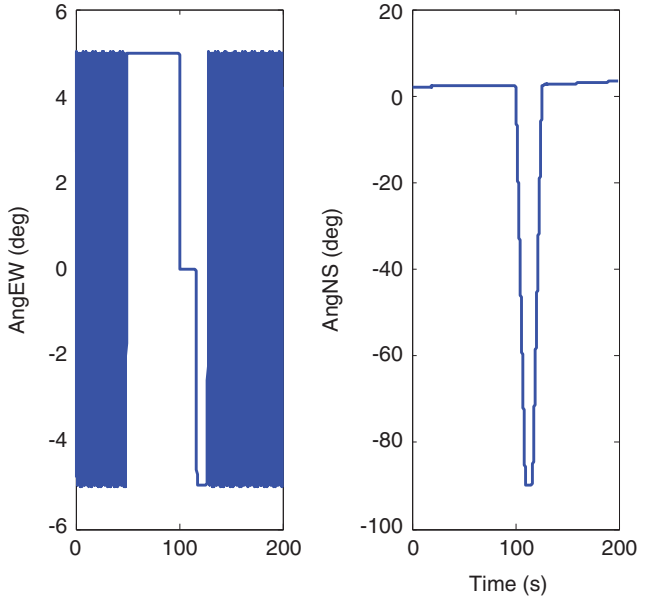

Fig. 5 Angular motion of the scanning mirror in the multichannel scanning radiometer (AngEW, angle of the east-west mirror; AngNS, angle of the north-south mirror).

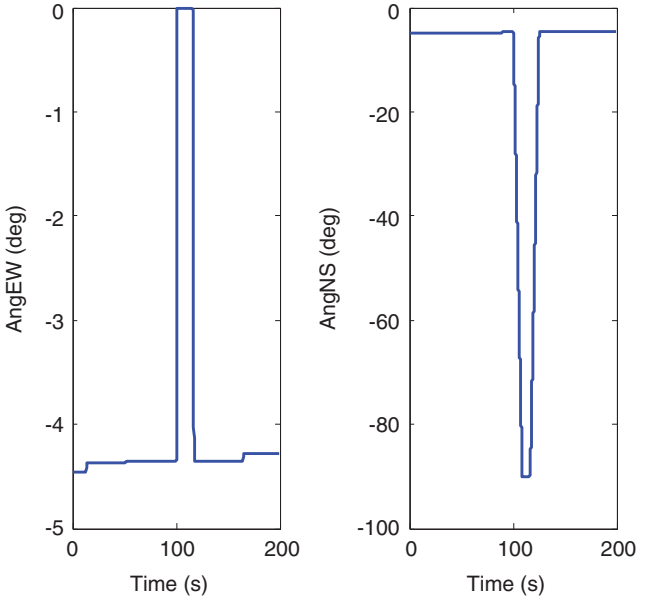

Fig. 6 Angular motion of the scanning mirror in the atmospheric sounding interferometer.

the data management computer as well as the feedforward torques generated by the attitude control system. The attitude control system compares the synchronization signals with the angular motions of the scanning mirrors computed for feedforward torques and accomplishes the time correction. The ground stations assess the feedforward control performance according to the attitude control errors acquired from the telemetry data and adjust the parameters of feedforward control if necessary.

In addition to the motion of payloads, the disturbance factors affecting the spacecraft stability include the driving torques generated by a solar array drive assembly and the flexible vibrations of the solar array. The frequencies of the driving torques is 0.1 Hz and its multiple. Their magnitudes are less than 0.05 N · m. Frequency isolation is adopted during the design phase to avoid the flexible appendage resonance, which could be excited by driving torques produced by the payloads or solar array drive assembly.

A physical simulation is undertaken to evaluate the pointing accuracy and stability of the Fengyun-4 attitude-pointing control

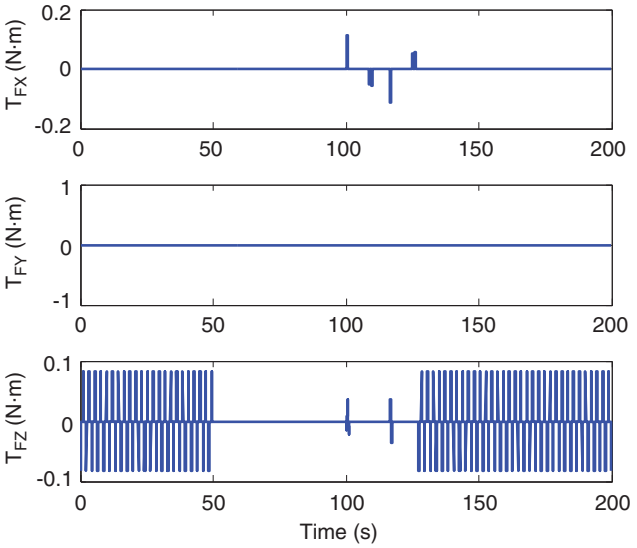

Fig. 7 Feedforward torques to compensate the disturbance of the payloads.

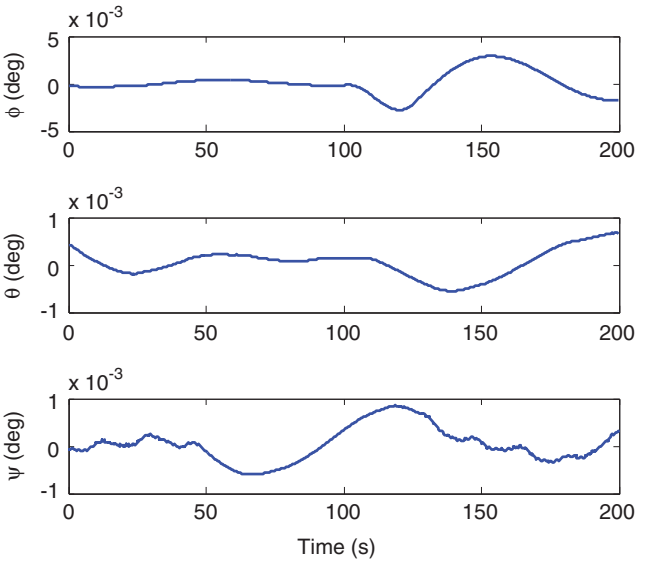

Fig. 8 Attitude-pointing errors during the payload moving.

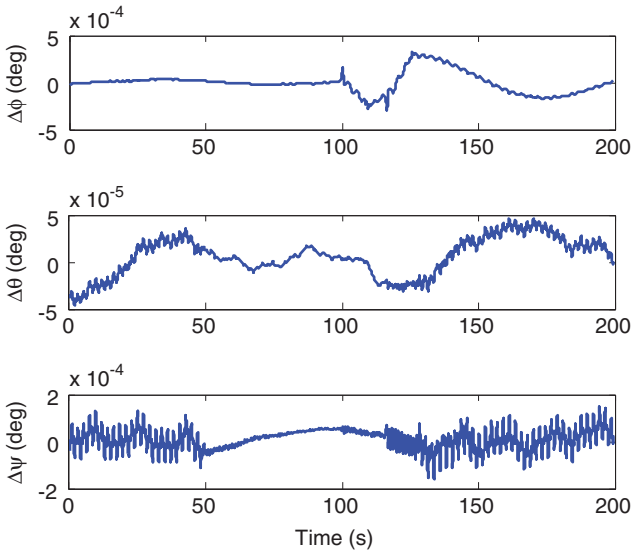

Fig. 9 Attitude integrated rate errors over 1 s during the payload moving.

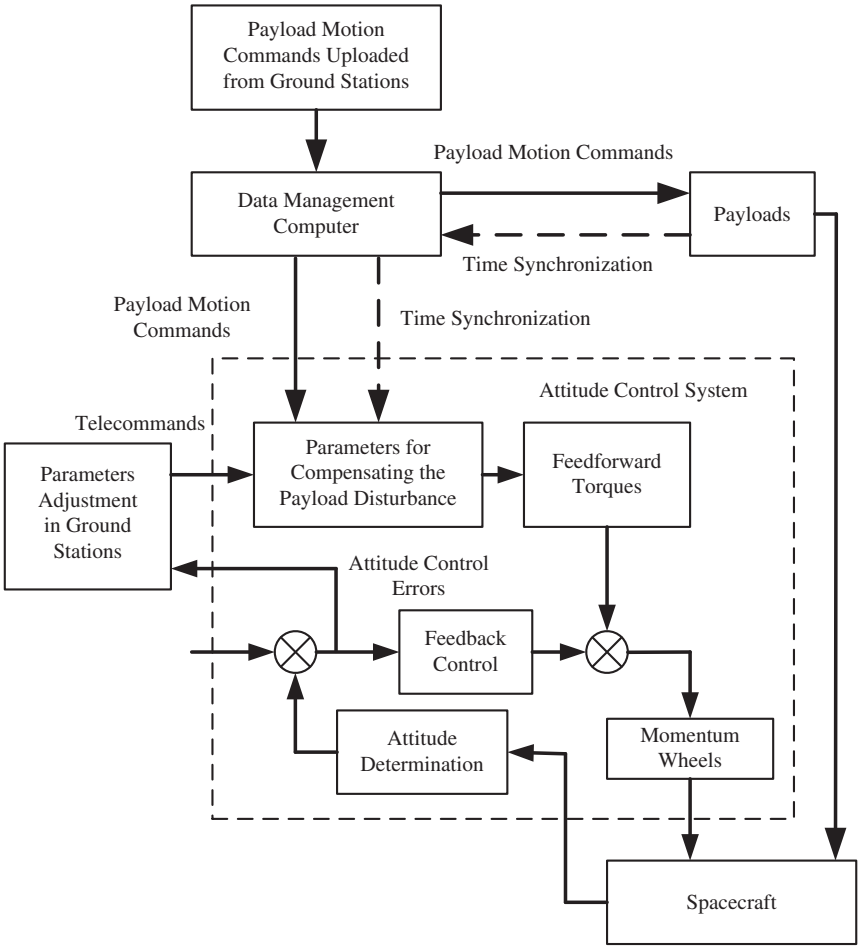

Fig. 10 Feedforward approach to compensate the disturbance torques generated by the payloads.

approach mentioned previously. A large three-axis air bearing system is used to simulate the spacecraft attitude motion. Devices produced for Fengyun-4 spacecraft, such as the onboard computer, the gyroscopes, the momentum wheels, the solar array drive assembly, and the payloads are installed on the three-axis air bearing system. A photoelectric autocollimator combined with a mathematical model is adopted to simulate the output of a star tracker. A rigid beam is fixed onto the output shaft of the solar array drive assembly to simulate the disturbance torques reacting on the spacecraft. Physical simulation results indicate that the attitude-pointing control approach of the spacecraft platform fulfills the mission requirements. The physical simulation results can be found in Figs. 11–13. A detailed description of the physical simulation can be found in [13].

C. Angular Momentum Management and Daily Adjustment

The Fengyun-4 spacecraft has a single solar array with an area of 17 m^2 on the $-Y$ panel and chooses a nadir-pointing reference attitude. The disturbance torque generated by the solar pressure has a daily period and results in the accumulation of angular momentum in the spacecraft momentum wheel system. The accumulated angular momentum could reach approximately 30 $N \cdot m \cdot s$ during a day in the inertial frame, and that fluctuates in the spacecraft body frame within a range of approximately 45 $N \cdot m \cdot s$. A momentum adjustment is required to avoid the spacecraft momentum wheels reaching the saturation. The meteorological operation is interrupted by the momentum adjustment because the attitude-pointing accuracy and stability of the spacecraft platform exceed the mission requirement when the 10 N thrusters operate. To reduce the amount of the momentum wheels and extend the meteorological operation time, a daily momentum adjustment is designed, and the time arranged for that operation is less than 15 min. A detailed discussion about the angular momentum management and adjustment can be found in [14].

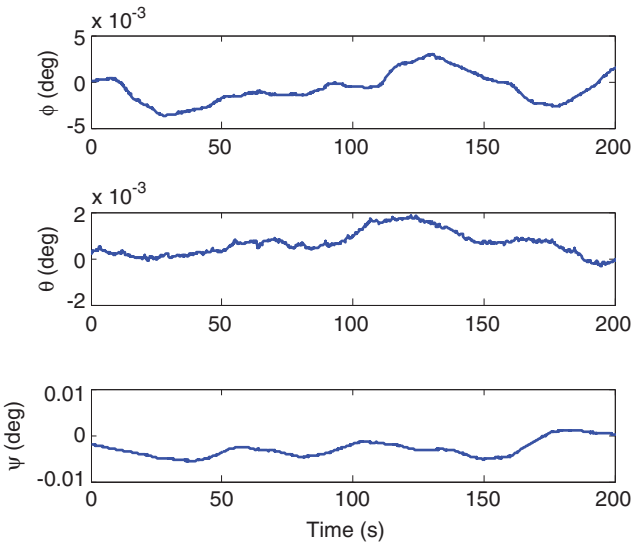

Fig. 11 Attitude-pointing errors during the payload moving.

The configuration of the momentum wheels is shown in Fig. 14. The axes of the six wheels are uniformly distributed around the $-Y_B$ axis of the spacecraft body frame and have a crossing angle of 75 deg with respect to the $-Y_B$ axis.

The speed of each momentum wheel is expected to vary between 500 and approximately 5100 rpm ($10.8 \sim 55.4$ $N \cdot m \cdot s$ in angular momentum) to avoid the resonance during low speed and the significant change of friction when the speed crosses zero. To solve that problem, the initial states in both the spacecraft angular

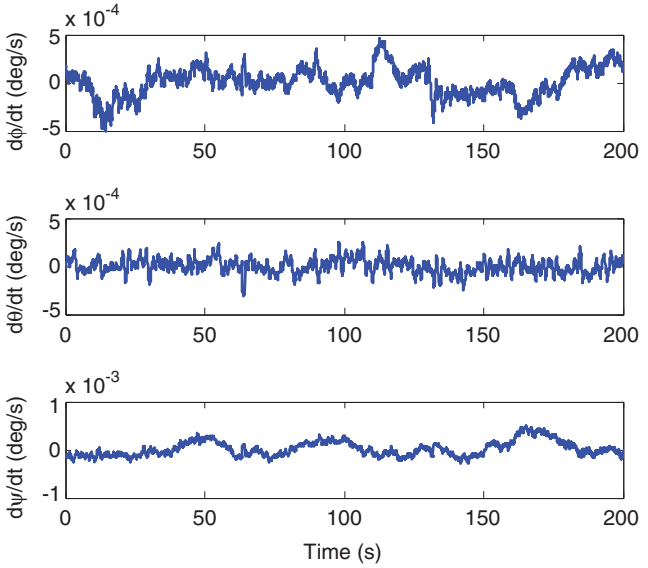

Fig. 12 Attitude rate errors during the payload moving.

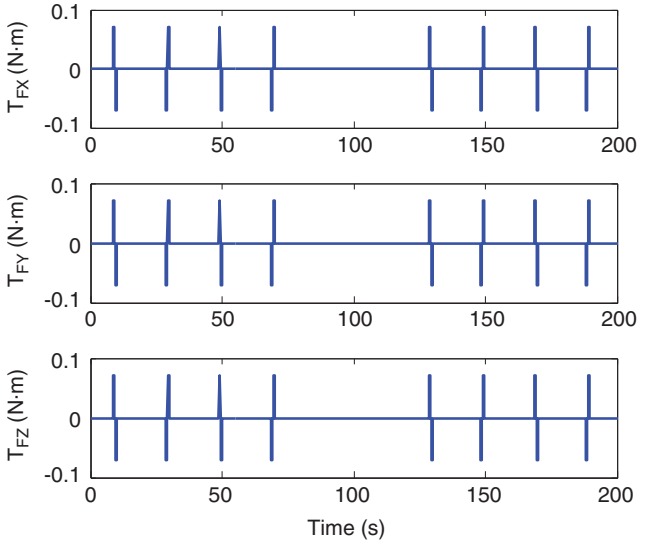

Fig. 13 Feedforward torques to compensate the disturbance of the payloads.

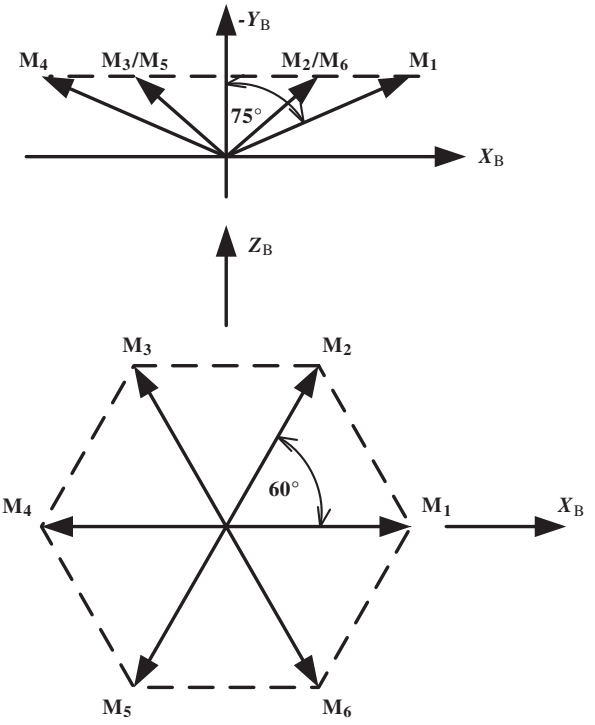

Fig. 14 Geometric representation of the momentum wheel configuration.

momentum space and the null space of the wheel assembly are investigated. It is known that the accumulation of the spacecraft angular momentum is mainly generated by the solar pressures and could be predetermined. The initial state in the spacecraft angular momentum space is set to half of the magnitude and opposite to its accumulated direction to minimize the magnitude of angular momentum accumulated in each axis during an orbital period. In the null space of the wheel assembly, the initial states of the momentum wheels are investigated in three conditions: 1) six working wheels, 2) five working wheels with one cold spare, and 3) four working wheels with two cold spares and three types (type K, type ψ, and type X, respectively; see Table 3). The initial states in the spacecraft angular momentum space are allocated to each wheel. Those initial states and the initial states in the null space of the wheel assembly constitute the preferred momenta of the wheels. A null motion steering command is used to make the momentum of each wheel approach the preferred state and satisfy the maximum torque of the wheels. The formulation is

$$\boldsymbol{T}_{\text{NullMW}} = -k(\boldsymbol{I}_{n\times n} - \boldsymbol{C}_{3\times n}^{T}(\boldsymbol{C}_{3\times n}\boldsymbol{C}_{3\times n}^{T})^{-1}\boldsymbol{C}_{3\times n})(\boldsymbol{h} - \boldsymbol{h}_{T}) \tag{4}$$

where $\boldsymbol{T}_{\text{NullMW}}$ is the command torque vector of the wheels for null motion steering, k is the adjustable parameter, $\boldsymbol{I}_{n\times n}$ is the identity matrix with a dimension of $n \times n$, $\boldsymbol{C}_{3\times n}$ is the angular momentum distribution matrix in the spacecraft body-fixed frame with a dimension of $3 \times n$, $\boldsymbol{h}$ is the measurement momenta of the wheels, and $\boldsymbol{h}_T$ is the preferred momenta of the wheels.

Daily momentum adjustment in the Fengyun-4 spacecraft is implemented by 10 N thrusters. During adjustment, the output of the thrusters is comprised by some fixed-width pulses and fixed-width intervals, alternately, according to the difference between the measured momentum of the spacecraft and the preferred state. During that process, the momentum wheels are used to keep the spacecraft pointing to Earth by the composite control method and to absorb the angular momentum generated by the thrusters to unload the accumulated angular momentum.

The time to adjust the spacecraft angular momentum could be designed to make the increment velocity generated by thrusters along the X axis of the spacecraft body frame equal to that required for east–west station keeping during an orbital period. This method could reduce the fuel consumption and the times used for east–west station keeping. Four momentum adjustment thrusters are installed along the X axis of the spacecraft body frame and can produce the force along the X axis and the torque along the Z axis. The formula used to determine the adjusting time can be expressed as

$$\frac{F_x \Delta H|\cos\varphi_M|}{T_z m} = \frac{v_s T}{3\omega_e}\ddot{\lambda}_s \tag{5}$$

Table 3 Initial-state vector in the null space of the wheel assembly

Mount of wheels	Serial number	Initial-state vector in the null space
6	123456	[−1, 1, −1, 1, −1, 1]
5	12345, 12346, 12356, 12456, 13456, 23456	[−3, 2, 2, −5, 4]
4	Type K (1234, 1456, 3456, 1236, 2345, 1256)	[−1, 2, −2, 1]
	Type ψ (1235, 1246, 1345, 1356, 2346, 2456)	[−1, 2, −3, 2]
	Type X (1245, 1346, 2356)	[1, −1, 1, −1]

Note: The serial number 1, 2, 3, 4, 5 and 6 refers to the momentum wheel M1, M2, M3, M4, M5 and M6 in Fig. 14 respectively.

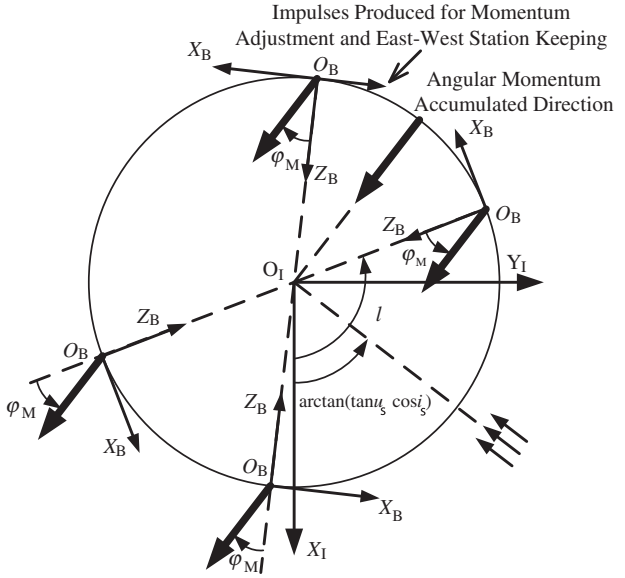

Fig. 15 Momentum adjustment associated with east–west station keeping.

where ΔH is the projection of the daily accumulated angular momentum on the orbital plane, F_x is the force along the X axis of the spacecraft body frame produced by the adjustment thrusters, T_z is the torque along the Z axis of the spacecraft body frame produced by the adjustment thrusters, φ_M is the angle between the accumulated direction of the angular momentum and the $+Z$ axis of the spacecraft body frame, m is the mass of the spacecraft, v_s is the specific velocity of the spacecraft in the geostationary orbit, T is the spacecraft orbital period, and $\ddot{\lambda}$ is the acceleration of the spacecraft mean longitude generated by nonspherical gravity. Therefore, the sidereal hour angles for momentum adjustment can be calculated as

$$l = \begin{cases} \arctan(\tan u_s \cos i_s) + \pi/2 + \varphi_M \\ \arctan(\tan u_s \cos i_s) + \pi/2 - \varphi_M \\ \arctan(\tan u_s \cos i_s) + 3\pi/2 + \varphi_M \\ \arctan(\tan u_s \cos i_s) + 3\pi/2 - \varphi_M \end{cases} \tag{6}$$

where i_s and u_s are the orbital inclination and the argument of latitude in the geocentric equatorial inertial coordinate frame, respectively. As shown in Fig. 15, the daily momentum adjustment associated with the east–west station keeping can be operated in four locations.

D. Attitude Capture with Star Trackers

To make the control system reliable and safe, the attitude control system of the Fengyun-4 spacecraft uses the output of the star trackers to determine its initial attitude and then maintains its attitude towards the sun, Earth, or any directions in the inertial frame. The attitude capture method is used in the geosynchronous transfer orbit before the orbital maneuvering at the apsis. The rotation of the spacecraft attitude is first damped by the thrusters. After the attitude has been stabilized, the outputs of the three star trackers are validated separately or interactively. Once the validity of those outputs is confirmed, the initial attitude could be determined. An attitude maneuver about the Euler axis of rotation is adopted to transform the initial attitude into the inertial attitude, the sun-pointing attitude, or the Earth-pointing attitude. If the outputs are invalid, then the spacecraft would be forced to rotate to a new stabilized attitude. After changing the orientation of the star trackers in the inertial frame, the outputs of the star trackers are reexamined.

E. Accommodation to Operate After Turning 180 deg About Yaw Axis

The $+Y$ panel of the Fengyun-4 spacecraft is selected as the radiant cooling panel. Therefore, the exposure of this panel to the sun should be avoided. For that reason, the spacecraft should maintain a 0 or 180 deg attitude along the yaw axis. During the time from the spring equinox to the autumnal equinox, the spacecraft adopts a forward attitude with the $+X$ axis of the spacecraft body frame pointing to the east and the $+Y$ axis pointing to the south. During the time from the autumnal equinox to the spring equinox in the next year, the spacecraft adopts a reverse attitude with the $+X$ axis pointing to the west and the $+Y$ axis pointing to the north. The yaw flip maneuvers are required twice a year. To accommodate that reverse attitude, the attitude determination strategy, the momentum management, and the adjustment strategy, as well as the thruster control strategy for the east–west station keeping, are modified.

F. Autonomous Fault Diagnosis and Disposition

The Fengyun-4 spacecraft is required to operate continuously and steadily and maintain its Earth-pointing attitude as long as possible. The attitude control system is capable of autonomously locating and isolating its faults as well as recovering. The fault diagnosis and disposition mainly focus on the fault of a single device. When multiple faults occur, it is necessary to locate the faults within the specific devices.

The optical sensors, such as the Earth sensors, the sun sensors, and the star trackers, could have various types of faults caused by device failures and the disturbance of sunlight, moonlight, and the Earth atmosphere reflected light, as well as strong light reflected by protuberances on the spacecraft. The attitude control system compares the current measurement information of the optical sensors with the past information. If the difference between those two pieces of measurement information exceeds a certain value, the optical sensor is regarded as disabled, and then a cold spare device or other methods will be used. When those faults occur, the accuracy of the attitude determination is degraded, and the fuel consumption of the thrusters is increased. The method to handle those faults is switching to a cold spare device or using other attitude determination methods.

The faults among the gyroscopes are determined by the correlated measurement equations. The logic sequence of the fault diagnosis is designed based on the number of gyroscopes employed by the attitude control system in real time. A fault diagnosis algorithm of five gyroscopes based on the vectors in null space is used when five or more gyroscopes are used. A fault among the five gyroscopes could be determined by projecting their measurements onto the two optimal orthogonal vectors in the null space of the five-gyroscopes configuration and comparing the magnitude of the projections with the precalculated thresholds. Once the fault among the five gyroscopes is determined, the fault could be located by projecting every four measurements of the gyroscopes on the two optimal orthogonal vectors in the null space of their configuration, and comparing the magnitude of the projections with the precalculated thresholds after excluding the uncertain gyroscopes.

The faults of actuators, such as thrusters and momentum wheels, could also be determined by physical characteristics when they are operated. A cold spare will be used when any of the actuators is regarded as disabled.

IV. In-Flight Performance of Fengyun-4 Attitude Control System

The Fengyun-4 attitude control system of the spacecraft platform fulfilled its requirements during the five orbit maneuvers at the apsis and the two maneuvers for phase capturing in quasi-geosynchronous orbit. After Fengyun-4 entered the geostationary orbit, the Earth-pointing control of the spacecraft platform with high accuracy and stability was achieved by feeding forward the disturbance torques generated by the scanning mirrors of the payloads. The momenta of the wheels were managed during an orbital period and adjusted once a day. The yaw flip maneuver was accomplished near the spring equinox, and the attitude control system was verified to operate in both the forward and reverse attitudes.

The in-flight performance of the feedforward control strategy was assessed on 28 December 2016 Coordinated Universal Time (UTC). The telemetry results during that time are present in Figs. 16–20. As shown in Figs. 16 and 17, the scanning mirrors in both the multichannel scanning radiometer and the atmospheric sounding interferometer had

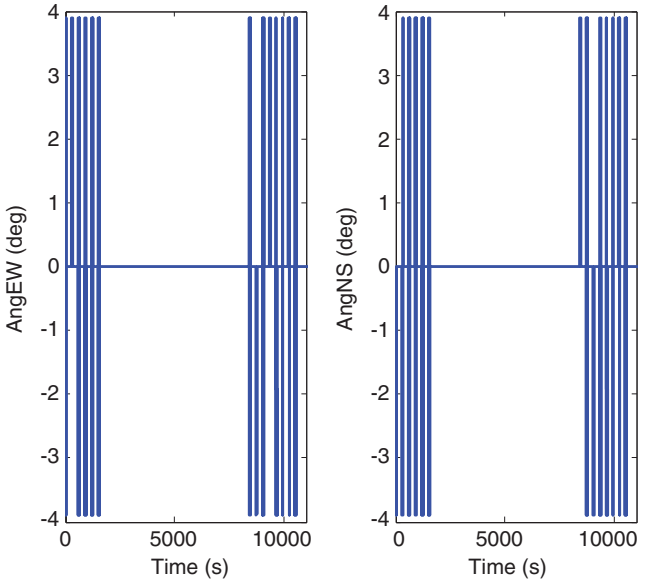

Fig. 16 Angular motion of the scanning mirror in the multichannel scanning radiometer.

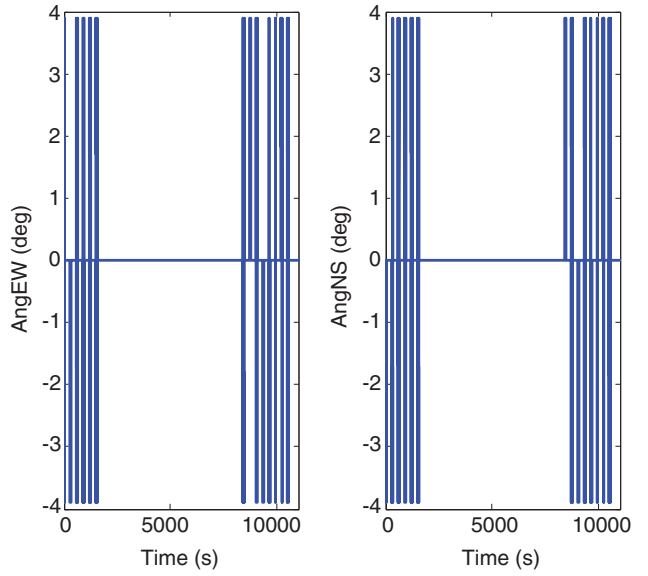

Fig. 17 Angular motion of the scanning mirror in the atmospheric sounding interferometer.

fast pointing motions during the two segments, $0 \sim 2000$ s and $8000 \sim 11{,}000$ s, respectively. The output torques of the working wheels (The serial numbers 1, 2, 4, and 5 refer to the momentum wheel M1, M2, M4, and M5 in Fig. 14 respectively.) are present in Fig. 18. It is worth noting that the feedforward torques for compensation were only adopted during the last segment (8000 s $\sim$ 11,000 s). The attitude control errors of the spacecraft platform and its attitude integrated rate errors over 1 s during those payloads moving are present in Figs. 19 and 20. The attitude control errors were less than 2×10^{-3} deg (see Fig. 19). The fast pointing motions of those scanning mirrors in both the multichannel scanning radiometer and the atmospheric sounding interferometer had a significant impact on the stability of the roll axis and the yaw axis (see Fig. 20). Its attitude integrated rate errors over 1 s during the first segment (0–2000 s) reached 0.0011 deg, which exceeded the mission requirement. In contrast, those errors in the last segment (8000–11,000 s) reached 0.0004 deg because the feedforward torques were adopted to compensate the payload disturbance angular momentum. Those results suggest that the feedforward control strategy is valid. The Earth-pointing accuracy and stability of the spacecraft platform fulfilled the mission requirements.

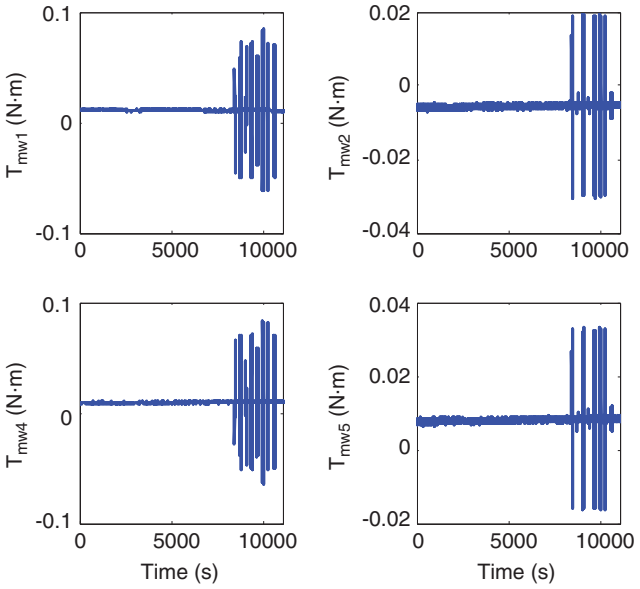

Fig. 18 Output torques to compensate the disturbance of the payloads.

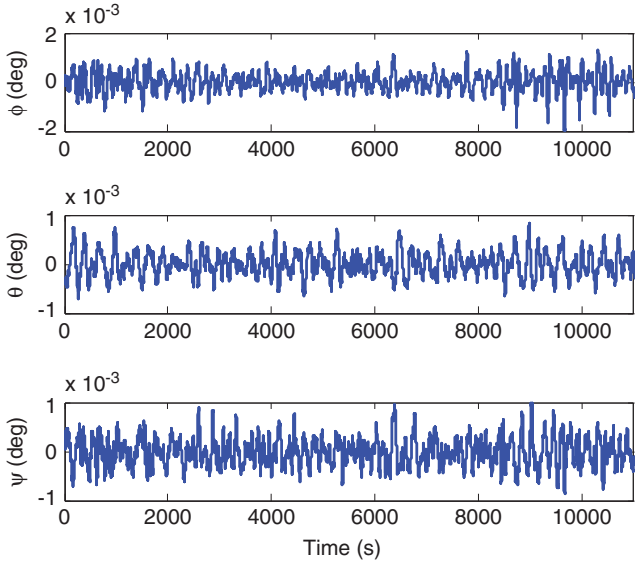

Fig. 19 Attitude-pointing control errors during the payloads moving.

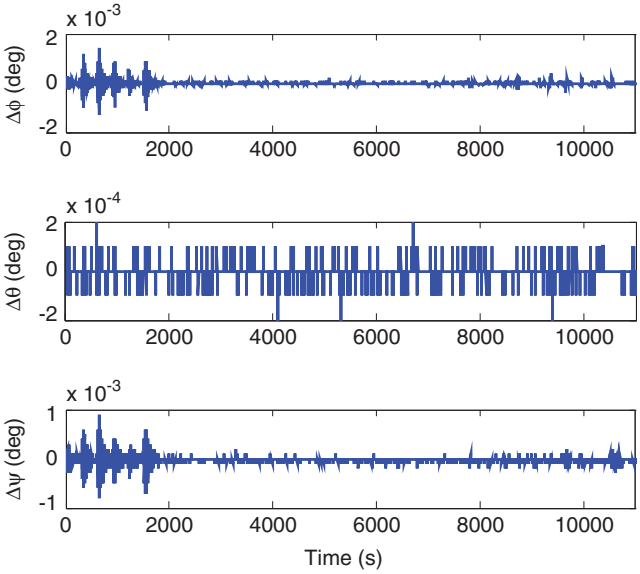

Fig. 20 Attitude integrated rate errors over 1 s during the payloads moving.

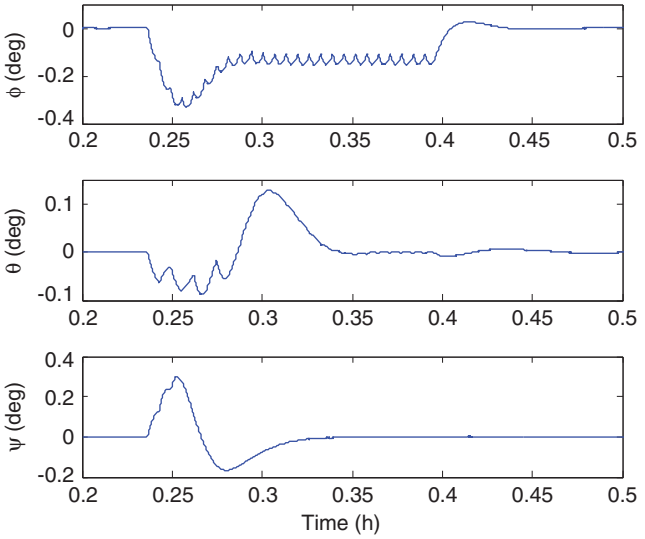

Fig. 21 Attitude errors during angular momentum adjustment.

The time appointed for the autonomous daily momentum adjustment is 00:00 in the spacecraft local time. The attitude errors and attitude rate errors of the spacecraft platform during the momentum adjustments at approximately 17:00 on 7 March 2017 (UTC) are shown in Figs. 21 and 22, respectively. During that time, the momentum of the wheel assembly absorbed from the solar pressure is mainly along the X axis of the spacecraft body frame. A thruster along the Z axis of the body frame that generates the torque along the X axis is mainly used to unload the momenta of the wheels. The telemetry results indicate that the adjusting thruster has a considerable impact on the spacecraft Earth-pointing accuracy and stability, especially along the X axis. The convergence time of the momentum adjustment is 11.753 min, less than the mission requirement of 15 min.

A yaw flip maneuver was accomplished on 20 March 2017 (UTC). The spacecraft adopted a reverse attitude with its $+X$ axis pointing toward the west before the maneuver and used a forward attitude with its $+X$ axis pointing toward the east after the maneuver. The momenta projected onto the X–Z plane in the spacecraft body frame before and after that maneuver are shown in Fig. 23. It can be found that the accumulated momentum along the Z axis had an opposite sign after that maneuver because the reference angular velocity vector turned 180 deg in the spacecraft body frame. The angular momenta of the working wheels and their friction torques estimated onboard are shown in Figs. 24 and 25, respectively. The friction

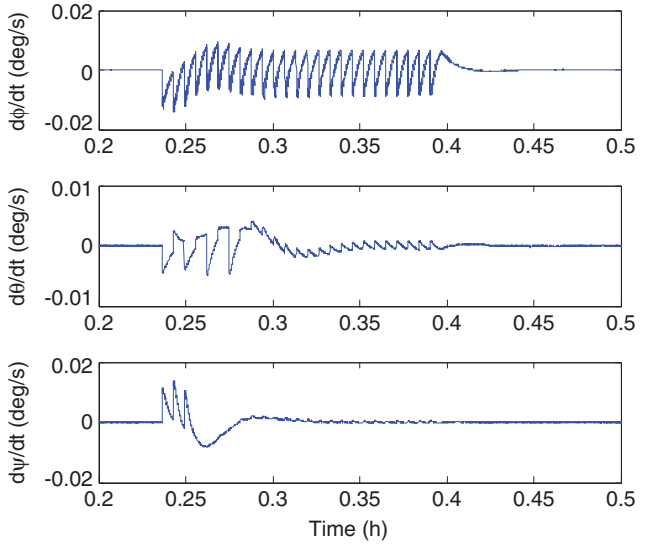

Fig. 22 Attitude rate errors during angular momentum adjustment.

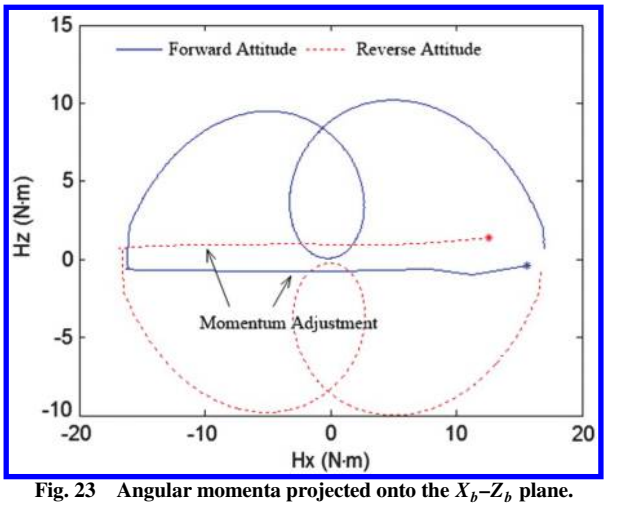

Fig. 23 Angular momenta projected onto the X_b–Z_b plane.

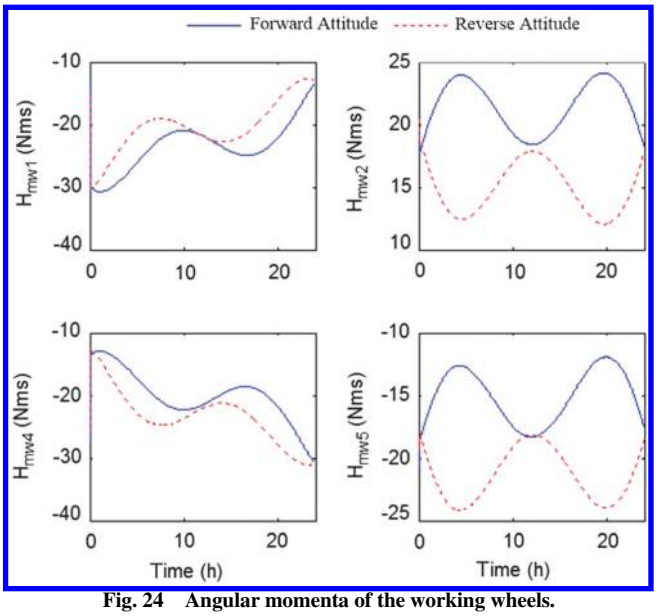

Fig. 24 Angular momenta of the working wheels.

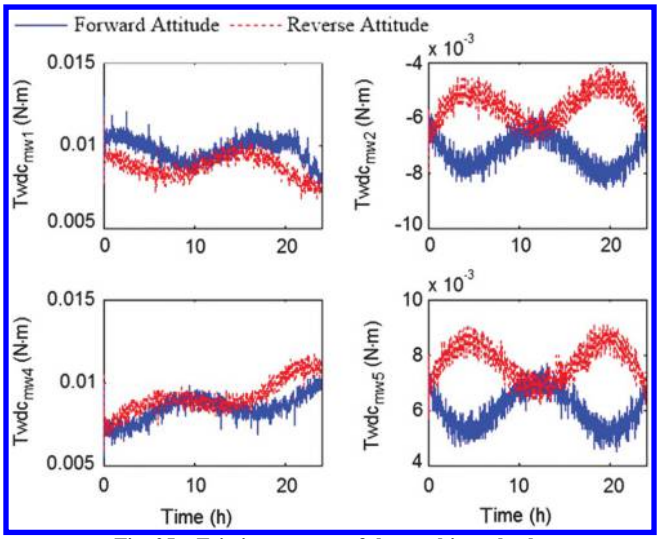

Fig. 25 Friction torques of the working wheels.

torques were estimated based on the measuring momenta of the wheels. The telemetry results suggest that the attitude control system is capable of managing the momentum of each working wheel and adjusting each momentum in a predetermined time. The speeds of the

wheels vary in the preferred range and avoid crossing zero or reaching saturation. The control system can accommodate the forward and reverse attitude control.

V. Conclusions

This Paper presented the composition and the specific techniques in the Fengyun-4 attitude control system of the spacecraft platform. The highly accurate attitude determination method and the attitude-pointing control method with high accuracy and stability requirements under the disturbance of rapid steering payloads were employed. The Earth-pointing accuracy of the spacecraft platform was able to reach to 0.01 deg, and its stability integrated over 1 s was less than 5×10^{-4} deg. The angular momentum of each wheel was managed and adjusted daily in a predetermined time. The attitude disturbance induced by the zero crossing or the saturation of the wheels was prevented. The momentum adjustment using the thrusters interrupted the meteorological observation. That time was less than 15 min. The adaptive design for working in a reverse attitude as well as autonomous fault diagnosis and disposition are used to ensure that the attitude control system could operate continuously and steadily. The in-flight results obtained from the telemetry suggest that the Fengyun-4 attitude control system of the spacecraft platform satisfies the requirement of the second generation of Chinese geostationary meteorological satellites.

Acknowledgments

This work was performed at Beijing Institute of Control Engineering. The authors acknowledge many individuals who contributed to the Fengyun-4 attitude control system of the spacecraft platform as well as the associate editor and the reviewers for their helpful suggestions and revisions to improve this Paper.

References

[1] Dond, Y. H., "FY-4 Meteorological Satellite and Its Application Prospect," *Aerospace Shanghai*, Vol. 33, No. 2, 2016, pp. 1, 8. doi:10.19328/j.cnki.1006-1630.2016.02.001

[2] Chapel, J., Stancliffe, D., Bevacqua, T., Winkler, S., Clapp, B., Rood, T., Gaylor, D., Freesland, D., and Krimchansky, A., "Guidance, Navigation, and Control Performance for the GOES-R Spacecraft," *CEAS Space Journal*, Vol. 7, No. 2, 2015, pp. 87–104. doi:10.1007/s12567-015-0077-1

[3] Chapel, J., Stancliffe, D., Bevacqua, T., Winkler, S., Clapp, B., Rood, T., Freesland, D., Reth, A., Early, D., and Walsh, T., et al., "In-Flight Guidance, Navigation, and Control Performance Results for the GOES-16 Spacecraft," *GNC2017: 10th International ESA Conference on Guidance, Navigation and Control Systems*, ESA, 2017, pp. 1–25.

[4] Griffith, P., "Advanced Himawari Imager (AHI) Design and Operational Flexibility," *12th Annual Symposium on New Generation Operational Environmental Satellite Systems*, American Meteorological Soc., 2016, pp. 1–24, https://ams.confex.com/ams/96Annual/webprogram/Handout/Paper289069/NGOESS-7.1_Griffith_AHI_Design_v2.pdf.

[5] Bessho, K., Date, K., Hayashi, M., Ikeda, A., Imai, T., Inoue, H., Kumagai, Y., Miyakawa, T., Murata, H., and Ohno, T., et al., "An Introduction to Himawari-8/9—Japan's New-Generation Geostationary Meteorological Satellites," *Journal of the Meteorological Society of Japan*, Vol. 94, No. 2, 2016, pp. 151–183. doi:10.2151/jmsj.2016-009

[6] "Himawari-8/9," http://spaceflight101.com/spacecraft/himawari-8-and-9/ [retrieved 29 March 2017].

[7] Tanguy, P., Smolders, A., Miesner, T., and Neri, E., "Meteosat Third Generation: Program Overview and Challenges," *63rd International Astronautical Congress*, International Astronautical Federation, 2012, pp.1–8, http://iafastro.directory/iac/paper/id/13258/abstract-pdf/IAC-12,B1,2,2,x13258.brief.pdf?2012-06-15.09:40:07.

[8] "Meteosat Third Generation—Next Generation Weather Satellites," https://www.ohb-system.de/tl_files/system/images/mediathek/downloads/pdf/OHB-System_MTG_2018.pdf [retrieved 29 March 2017].

[9] Lyu, W., Dai, S. L., Dong, Y. H., Shen, Y. L., Song, X. Z., and Wang, T. S., "Attitude Motion Compensation for Imager on Fengyun-4 Geostationary Meteorological Satellite," *Acta Astronautica*, Vol. 138, Sept. 2017, pp. 290–294. doi:10.1016/j.actaastro.2017.05.033

[10] Dong, Y. H., Zhou, X. B., Shen, J. F., Liu, X. T., and Yu, Z. F., "Study on Micro-Vibration Suppression Technology of FY-4 Satellite," *Aerospace Shanghai*, Vol. 34, No. 4, 2017, pp. 20–27. doi:10.19328/j.cnki.1006-1630.2017.04.003

[11] Liu, Y. W., and Chen, Y. Q., "Star-Sensor Measurement Model and its Application to the Spacecraft Attitude Determination System," *Journal of Astronautics*, Vol. 24, No. 2, 2003, pp. 162–167. doi:10.3321/j.issn:1000-1328.2003.02.009

[12] Xiong, K., Tang, L., and Liu, Y. W., "Calibration of Star Sensor's Low Frequency Error Based on Landmark Information," *Aerospace Control and Application*, Vol. 38, No. 2, 2012, pp. 11–15. doi:10.3969/j.issn.1674-1579.2012.03.003

[13] Chen, S. L., Wang, Z. W., Liu, Y. W., and Mu, X. G., "Physical Simulation of the Control System in the New Generation Geostationary Meteorological Satellite," *21st Academic Conference of Space Exploration Committee of the Chinese Society for Space Research*, Chinese Soc. for Space Research, 2008, pp. 58–64, http://www.wanfangdata.com.cn/details/detail.do?_type=conference=6862485.

[14] Liu, Y. W., Si, Z. H., Tang, L., and Chen, S. L., "Angular Momentum Management Strategy of the FengYun-4 Meteorological Satellite," *Acta Astronautica*, Vol. 151, Oct. 2018, pp. 22–31. doi:10.1016/j.actaastro.2018.05.031

E. G. Lightsey
Associate Editor